

Supporting Information

Cell penetrating peptide induces self-reproduction of phospholipid vesicles: understanding the role of bilayer rigidity

Pavel Banerjee, Siddhartha Pal, Niloy Kundu, Dipankar Mondal and Nilmoni Sarkar*

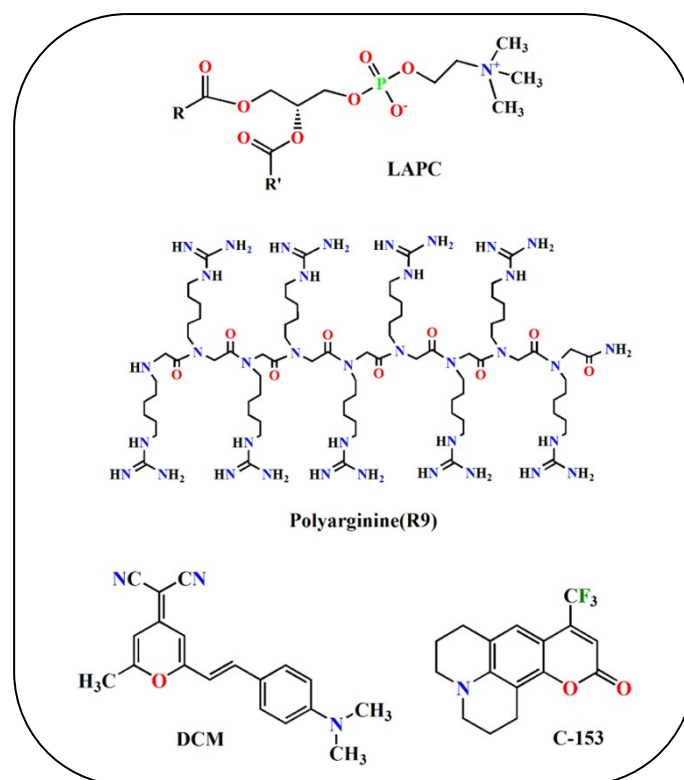
Department of Chemistry, Indian Institute of Technology, Kharagpur 721302, WB, India

E-mail: nilmoni@iitkgp.ac.in, nilmonisarkar1208@gmail.com

Table of contents

1. Materials and Sample Preparation	S2
2. Instrumentations	S3
3. Tables	S7
4. Figures	S8
5. References	S16
6. Movie 1	

1. Materials and Sample Preparation: LAPC (L- α -Phosphatidylcholine), Coumarin-153 (C-153) were purchased from Sigma Aldrich and used as received. 4-(Dicyanomethylene)-2-methyl-6-(4-dimethylaminostyryl)-4H-pyran (DCM) dye was used as received from Exciton. The cell-penetrating peptide, nonaarginine (R9) was received from Novopep Limited. Throughout the experiments mili-Q water (ddH₂O) was used. The resistivity of the mili-Q water was 18.2 M Ω ·cm at 25 °C in our set up. The chemical structures of all the chemicals are shown in Scheme S1. All the spectroscopic grade solvents were obtained from Merck and used without further purification. Stock solution of R9 was prepared in phosphate buffer saline (PBS, 0.1 M, pH 7.4). For switching the pH to 5.6 and 8.0, we have used HCl and NaOH correspondingly. Vesicles were prepared following earlier reports.¹ Briefly a solution of each individual lipids in a 1:1(v/v) mixture of chloroform and methanol was slowly evaporated to produce a thin film on the inner surface of the round bottom (RB) flask. To the thin film of lipid solution PBS was added gently and the volume was adjusted to obtain the final concentration of lipid ~12 mM. We kept the vesicles solution under probe sonication for 10 minutes and then these solutions were passed through the 450 nm pore size cellulose filter paper to get uniformly distributed vesicles having average size ~100 nm vesicles (**see fig. S1,b**). Then the solutions were poured into the methanol evaporated DCM or C-153 (as required for the study).



Scheme S1. Chemical structures of LAPC, Polyarginine (R9), DCM and C-153.

2. Instrumentation.

2.1. Steady State Fluorescence Study. 4-(Dicyanomethylene)-2-methyl-6-(4-dimethylaminostyryl)-4H-pyran (DCM) was used as a probe to monitor steady state fluorescence studies. The concentrations of vesicle and DCM were maintained at 12 mM and 10 μ M, respectively. The fluorescence intensity of DCM was recorded using Shimadzu RF-6000 spectrofluorometer. The samples were excited at 488 nm. The slit width of the monochromator is 5/3 (excitation/emission) for all measurements.

2.2. Dynamic Light Scattering (DLS) and Zeta Potential (ζ) Measurements. To determine the size of the vesicles in absence and presence of R9, Malvern Nano ZS instrument with 4 mW He-Ne laser ($\lambda = 632.8$ nm) and thermostated sample holder was used. The same instrument was used for zeta potential (ζ) measurements. In this instrument, the detector angle was fixed at 173°. During DLS measurements, the collected scattering intensities were analyzed to calculate the hydrodynamic diameter (d_h) of particles using following equation:

$$d_h = \frac{k_B T}{3\pi\eta D} \quad (1)$$

where k_B , T , D and η denote Boltzmann constant, temperature, diffusion coefficient and viscosity, respectively. The details of this setup is already described in our earlier publication.²

2.3. Fluorescence Lifetime Imaging Microscope (FLIM) and Fluorescence Correlation Spectroscopy (FCS).

FLIM experiments were performed using a DCS-120 (Becker & Hickl GmbH) system equipped with an inverted optical microscope of Zeiss. For FLIM measurements, a 20 \times objective with numerical aperture (NA) 1.2 has been used. A diode laser at 488 nm, working at pulse mode (~ 20 mW), was used for sample excitations, and long pass filters (498 nm) were used to separate the fluorescence signal from the excitation source. The dye concentration of DCM was maintained as ~ 6 μ M for the FLIM measurements and it is done in solution phase. For FCS, a 40 \times objective is used. During FCS 488 nm diode laser was operated in the continuous wave (CW) mode. FCS measurements were performed with a hydrophobic dye. The calculated transverse radii (r) and the confocal volume were ~ 365 nm and 1.5 fL respectively of our experimental set-up. Epi-fluorescence was

collected and focused onto two avalanche photodiodes (APDs) (ID-Quantique ID100). Two APDs were used in order to eliminate all influence of the inherent noise, and after-pulsing effects of the detectors. The signal from the two APDs was analyzed by a PC-based correlator. Since in the case of FCS, a very small observation volume (in the order of femtoliter) is produced inside the sample, the probe was taken in nanomolar concentration, so that only one probe molecule was present in the observation volume. DCM was used as a fluorescent marker in both FLIM and FCS techniques. The details of the instrumentation and fitting were described in our earlier publication.^{2,3}

2.4. Transmission Electron Microscopy (TEM) Measurements. Transmission electron microscopy (TEM) analysis was carried out by using JEOL model JEM 2010 transmission electron microscope at an operating voltage 200 kV. TEM samples are prepared by blotting a carbon coated (50 nm carbon film) Cu grid (300 mesh, electron microscopy science) with a drop of solution and the samples are allowed to be dried for overnight.

2.5. Fluorescence Anisotropy Imaging Microscopy (FAIM) images and analysis.

The same FLIM set up was used as the basis for the measurement of rotational dynamics of DCM at the vesicle bilayer. Only change we made at the detection path (Diagram S1). We used a polarizing beam splitter at the detection path and signal was divided in a way that the horizontal polarization goes to the upper detector, and vertical polarization reflects down to the lower detector. But the contrast ratio is not perfect for two APD; there was difference of intensity of light in different channels for a symmetric fluorescent molecule. Therefore we have corrected the detection efficiency of two APD placed at the orthogonal to each other. G factor calibration for anisotropy measurement was performed using Perylene dye at room temperature at 298 K for 40X objective with 1.2 NA keeping same width of pinhole for parallel and perpendicular signal component. G is corrective factor defined as the ratio of detection efficiency for the parallel and perpendicular signal components. The fluorescence images at parallel, perpendicular direction and their anisotropy images were generated with MATLAB software after background subtraction. The final anisotropy image was smoothed by a uniform in build filter function using MATLAB. Background pixels were excluded by threshold masking. The mean $r(t)$ for each anisotropy image was calculated from the mean intensity-weighted pixel values. Measurements were performed at 298 K.

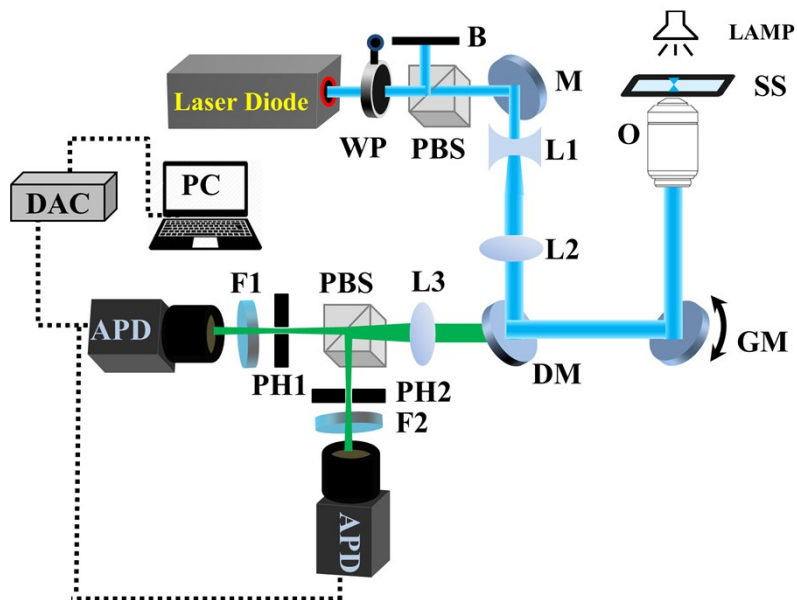


Diagram S1. : Optical diagram of fluorescence anisotropic imaging set up. WP: Half wave plate; M: Mirror; B: Blocker; L(1-3): Lens; DM: Dichroic mirror; GM: Galvanometer mirror; O: Objective lens; PH(1-2): PBS: Polarizing beam splitter; pinhole; F(1-2): Filters; APD: Avalanche photodiode; DAC: Data acquisition card; PC: personal computer; SS: sample stage; Lamp: White light source.

Anisotropy measurements were calculated using the following equation

$$r(t) = \frac{I_{\parallel} - I_{\perp}}{I_{\parallel} + 2I_{\perp}} \quad (2)$$

In the above equation, $r(t)$ is the measured anisotropy, and I_{\parallel}, I_{\perp} are the fluorescence emission intensities with polarization oriented parallel and perpendicular to that of a linearly polarized excitation beam respectively. The detector noise of two photodetectors was subtracted from the whole image before the data were processed.

2.6. Time Resolved Fluorescence Measurement:

The solvent reorganization time was measured using (TCSPC) instrument from IBH (U.K.). In our TCSPC set up, a picosecond diode laser (IBH, Nanoled) of 402 nm was used to excite the C-153 present in vesicle. The instrument response function of our setup was about 90 ps.

Decay kinetics were recorded from blue to red end keeping emission polarizer at magic angle (54.7°) using a Hamamatsu microchannel plate photomultiplier tube (3809U). The primary data consist of a set of emission decays recorded at a series of wavelengths spanning the steady-state emission spectrum. The time resolved emission spectra (TRES) ($S(\lambda, t)$), at a given time t , were obtained by spectral reconstruction, which is a relative normalization of the fitted decays, $D(t, \lambda)$ to the steady state emission spectrum $S_0(\lambda)$.

$$S(\lambda, t) = \frac{D(\lambda, t)S_0(\lambda)}{\int_0^{\infty} D(\lambda, t)dt} \quad (3)$$

Log-normal fitting of TRES yields various characteristic parameters, such as FWHM and emission maxima ($\nu(t)$) of TRES. For the construct of the decay of solvent correlation function $C(t)$, this peak frequency was used and $C(t)$ is defined as

$$C(t) = \frac{\nu(t) - \nu(\infty)}{\nu(0) - \nu(\infty)} \quad (4)$$

where $\nu(0)$, $\nu(t)$, and $\nu(\infty)$ are the peak frequencies at time zero, t , and infinity. The decays of $C(t)$ were fitted bi-exponentially using the following function

$$C(t) = \sum_{i=1}^n a_i \exp(-t/\tau_i) \quad (5)$$

Where “ τ ” is the solvation times with amplitudes of “ a ” and n is 2. The FWHM’s increased after the onset of excitation and reach a maximum at a time near to the average relaxation time, followed by a decrease. Solvent relaxation only would become slower than the fluorescence decay and thus cannot complete, only an increase of the FWHM would be observed. The same set-up was used during anisotropy measurement only a motorized polarizer was used on the emission side. The emission decays were collected at parallel $I_{\parallel}(t)$ and perpendicular $I_{\perp}(t)$ polarizations at regular time intervals until the desired peak difference between $I_{\parallel}(t)$ and $I_{\perp}(t)$ emission decays was reached. The following equation was used to measure $r(t)$.

$$r(t) = \frac{I_{\parallel} - GI_{\perp}}{I_{\parallel} + 2GI_{\perp}} \quad (6)$$

The correction factor, G , has been calculated using horizontally polarized excitation light. The horizontal (I_{\parallel}) and vertical (I_{\perp}) components of the emission decay were collected through the emission monochromator when the emission polarizer was fixed at horizontal and vertical

positions respectively. In our TCSPC setup, G value was estimated 0.6. TCSPC data analysis was performed using IBH DAS-6 decay analysis software.

2.7. Nuclear Magnetic Resonance (NMR) Measurements. The ^{31}P NMR of the LAPC vesicles in absence and presence of R9 were performed using Bruker 400 MHz NMR spectrometer. We studied all the NMR measurements in D_2O solvent (Cambridge Isotope Laboratories, 99.9 atom % D) which was used as chemical shift reference for mode locking.

2.8. Circular Dichroism (CD) Spectroscopy. The near-UV CD spectra were recorded at 298 K using a Jasco J-815 CD spectrometer. A quartz cuvette (path length 10 mm) was used for the measurements. The secondary structural changes, in the range of 190-250 nm, were recorded using a scan rate of 100 nm/ min; the final spectrum was averaged over three scans. Baseline subtractions were done with PBS for R9 in PBS and blank LAPC solution for R9 in LAPC to correct the obtained spectra. The vesicle concentration is diluted ~ 20 times to avoid scattering.

3. Supporting Tables.

Table S1. The diffusion parameters obtained by fitting the fluorescence correlation curves of DCM in LAPC Vesicle in the Presence and Absence of CPPs (R9) (30 μM)

System	$\tau_{\text{ves}}(\mu\text{S})$	$(D_t)_{\text{ves}}(\mu\text{m}^2 \text{S}^{-1})$	R^2
Only LAPC	4160 \pm 370	8.00 \pm 0.70	0.93
LAPC+ R9 – 3Day	2890 \pm 420	11.52 \pm 1.70	0.95

Table S2. Decay Parameters of C(t) of C153 in LAPC Vesicle in the Presence and Absence of CPPs (R9) (30 μM)($\lambda_{\text{ex}} = 402 \text{ nm}$)

System	$\tau_1(\text{nS}) (\%a_1)$	$\tau_2(\text{nS}) (\%a_2)$
Only LAPC	1.40 \pm 0.10(75%)	5.90 \pm 0.20(25%)
LAPC+ R9 – 3Day	1.10 \pm 0.03(80%)	3.80 \pm 0.30(20%)

Table S3. Time-Resolved Anisotropy Decay Parameters of C153 in LAPC Vesicle in the Presence and Absence of CPPs (R9) (30 μM) ($\lambda_{\text{ex}} = 402 \text{ nm}$)

System	$\tau_1(\text{nS}) (\%a_1)$	$\tau_2(\text{nS}) (\%a_2)$
Only LAPC	0.58 ± 0.02 (38%)	4.22 ± 0.30 (62%)
LAPC+ R9 – 3Day	0.47 ± 0.02 (45%)	3.30 ± 0.20 (55%)

4. Supporting Figures.

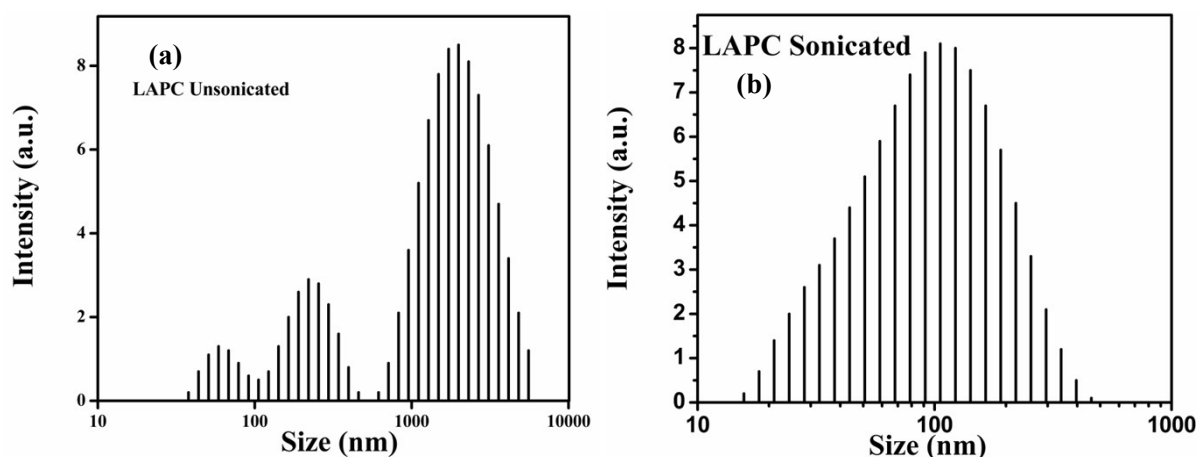


Fig. S1 DLS intensity versus size distribution histograms of LAPC Vesicles in (a) unsonicated and (b) sonicated forms.

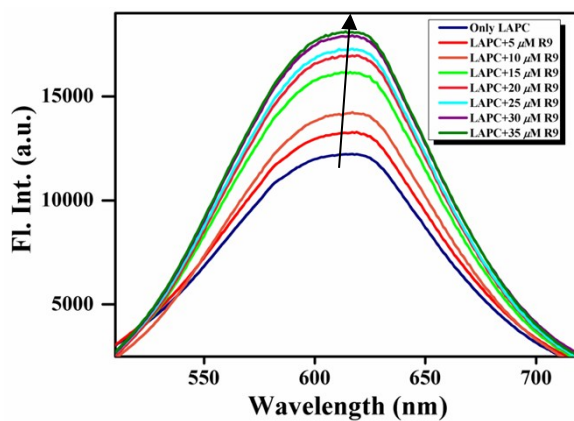


Fig. S2 Steady state emission spectra of DCM in LAPC Vesicles in presence of increasing concentration of R9.

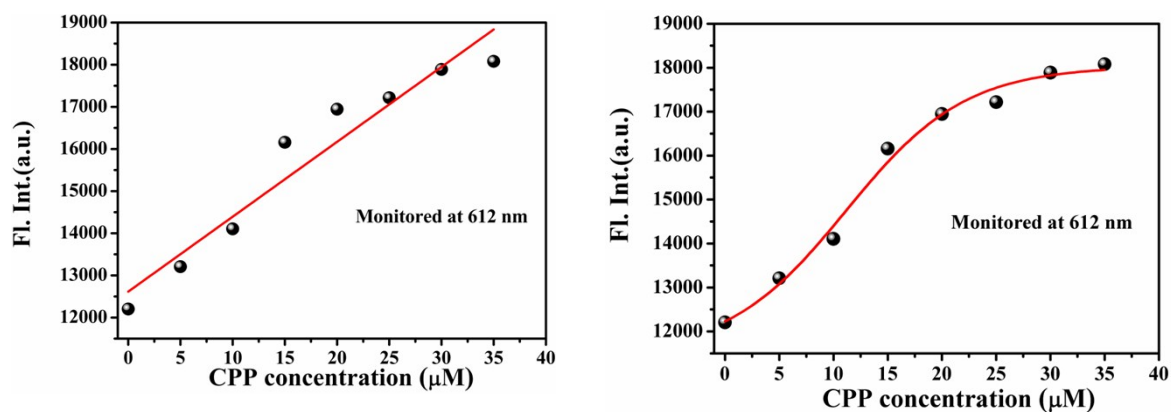


Fig. S3 Linear vs non-linear fitting of Steady state emission spectra of DCM in LAPC vesicles in presence of increasing concentration of R9 (monitored at 612 nm).

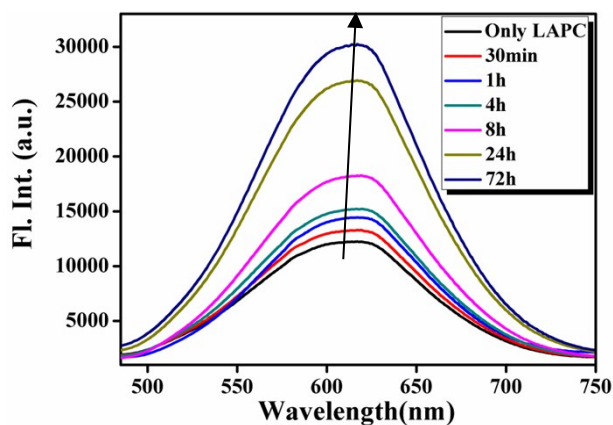


Fig. S4 Time dependent steady state emission spectra of DCM in LAPC Vesicles in presence of CPPs (R9) ($30 \mu\text{M}$).

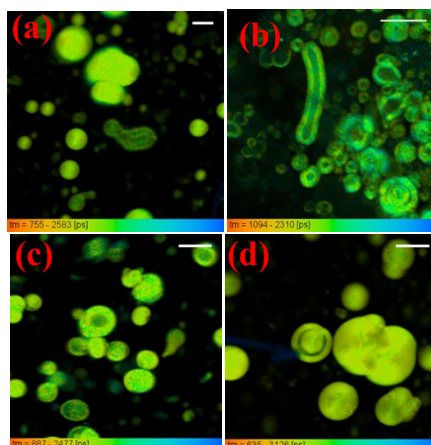


Fig. S5 FLIM images of different shapes obtained of LAPC vesicles after 1 hour of CPPs (R9) (30 μ M) addition (scale bar is 3 μ m).

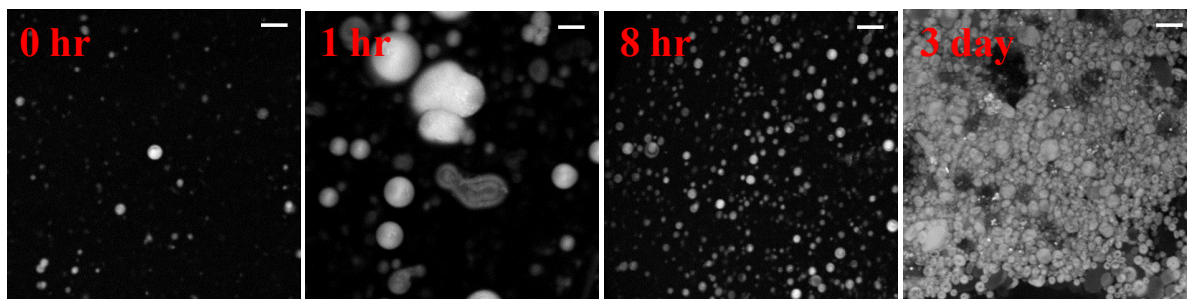


Fig. S6 Time dependent Intensity images of LAPC vesicles in presence of 30 μ M R9 (scale bar is 3 μ m).

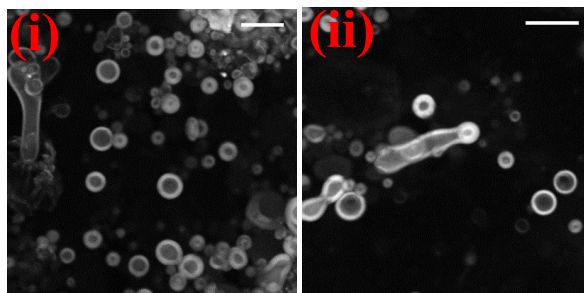


Fig. S7 Intensity images of LAPC vesicles after 3 days of CPPs (R9) (30 μ M) addition (scale bar is 3 μ m).

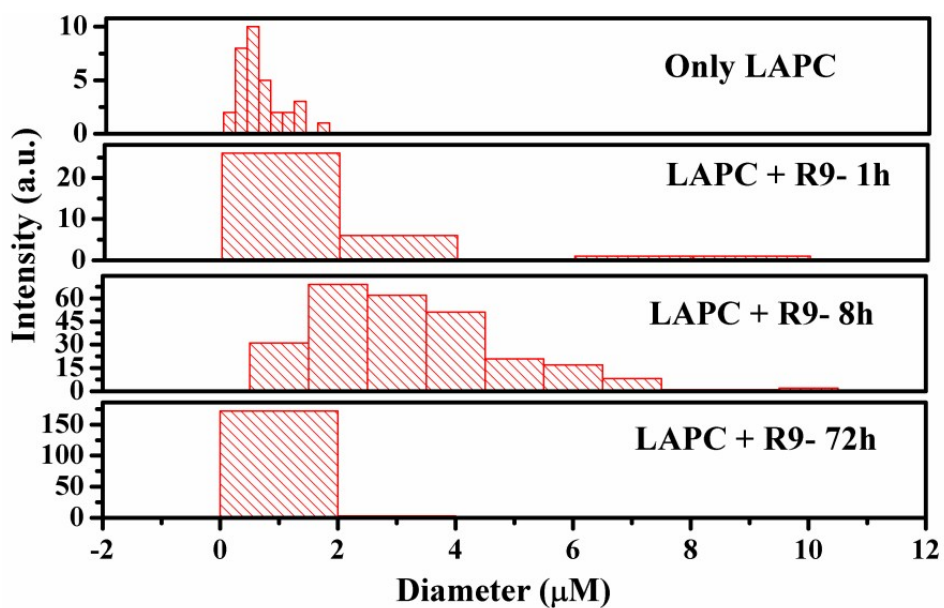


Fig. S8 Statistical analysis of FLIM images of LAPC vesicles in presence 30 μM R9 peptides (Corresponding images are in the manuscript, Fig 1-(d)).

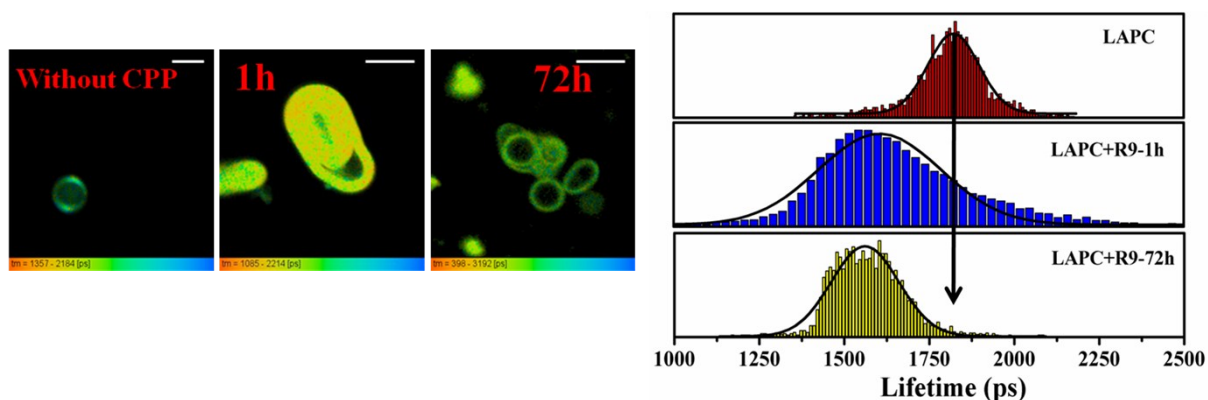


Fig. S9 Time dependent FLIM (scale bar 3 μm) images and lifetime distributions of LAPC vesicles in presence of 2 μM R9 peptides.

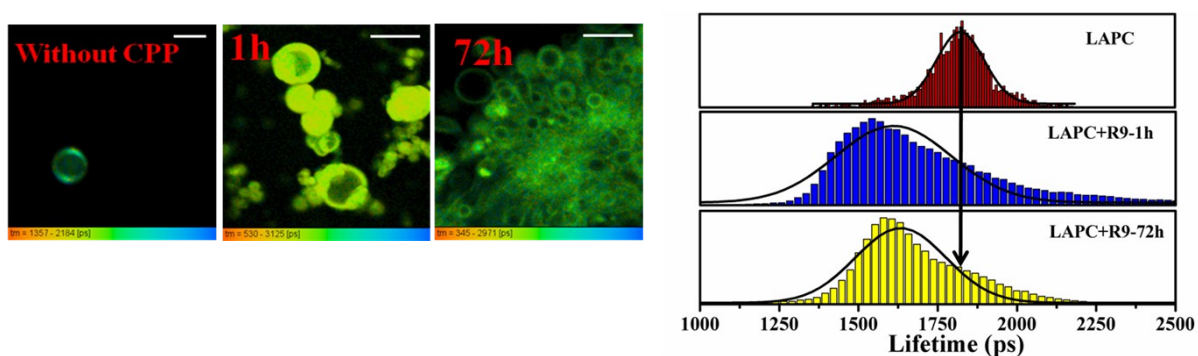


Fig. S10 Time dependent FLIM (scale bar 3 μm) images and lifetime distributions of LAPC vesicles in presence of 8 μM R9 peptides.

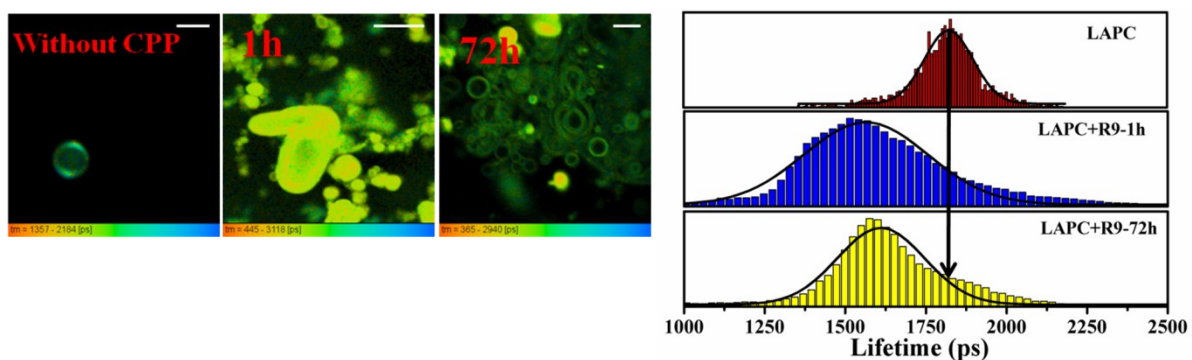


Fig. S11 Time dependent FLIM (scale bar 3 μ m) images and lifetime distributions of LAPC vesicles in presence of 20 μ M R9 peptides.

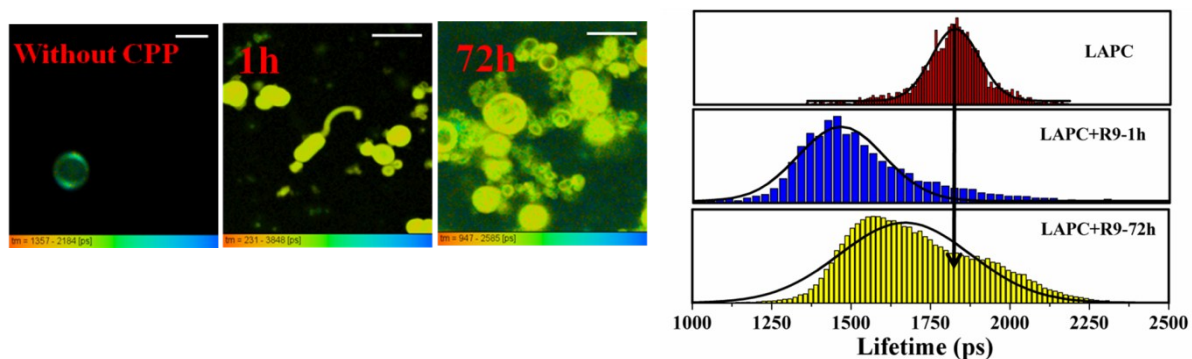


Fig. S12 Time dependent FLIM (scale bar 3 μ m) images and lifetime distributions of LAPC vesicles in presence of 27 μ M R9 peptides.

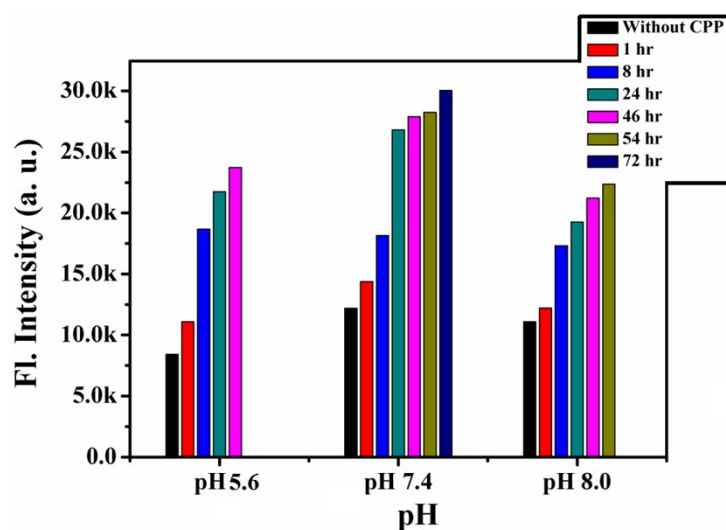


Fig. S13 Time dependent steady state emission spectra of DCM in LAPC Vesicles in different pH in presence of 30 μ M R9.

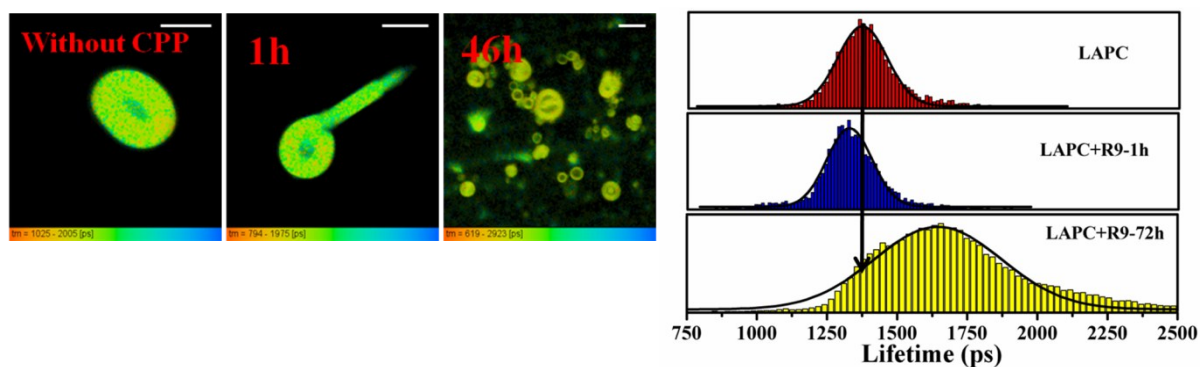


Fig. S14 Time dependent FLIM (scale bar 3 μm) images and lifetime distributions of LAPC vesicles at pH 5.6 in presence of 30 μM R9 peptides.

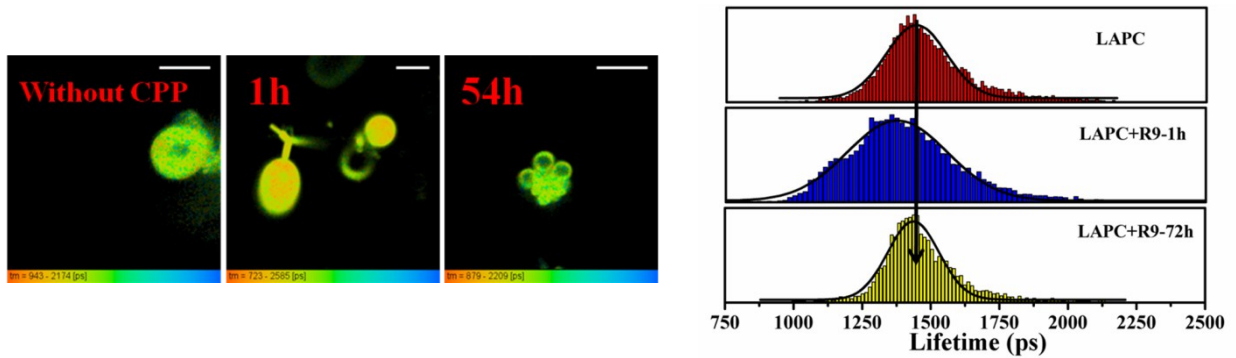


Fig. S15 Time dependent FLIM (scale bar 3 μm) images and lifetime distributions of LAPC vesicles at pH 8.0 in presence of 30 μM R9 peptides.

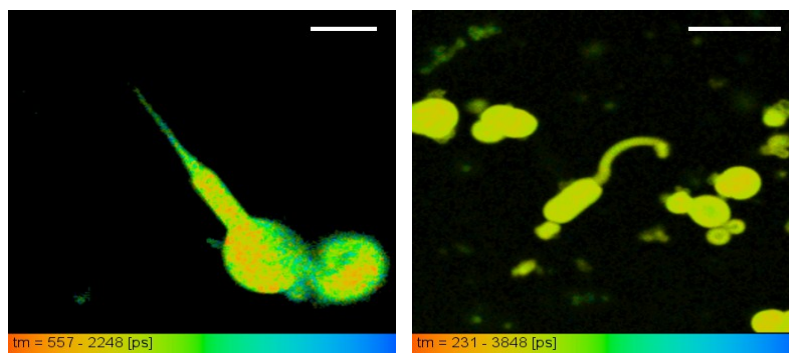


Fig. S16 FLIM (scale bar 3 μm) images of filamentous growth of LAPC vesicles in presence of R9 peptides.

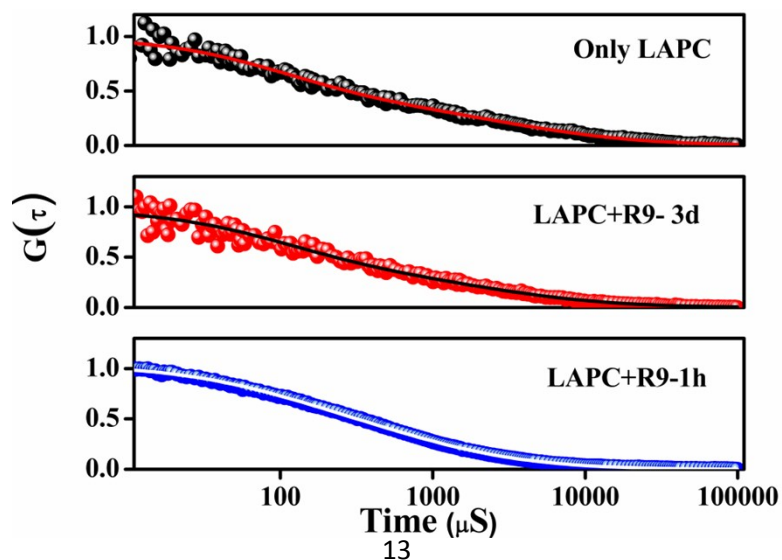


Fig. S17 FCS traces of DCM in LIPC Vesicles in absence and presence of CPPs (R9) (30 μ M) (1 hour and 3days).

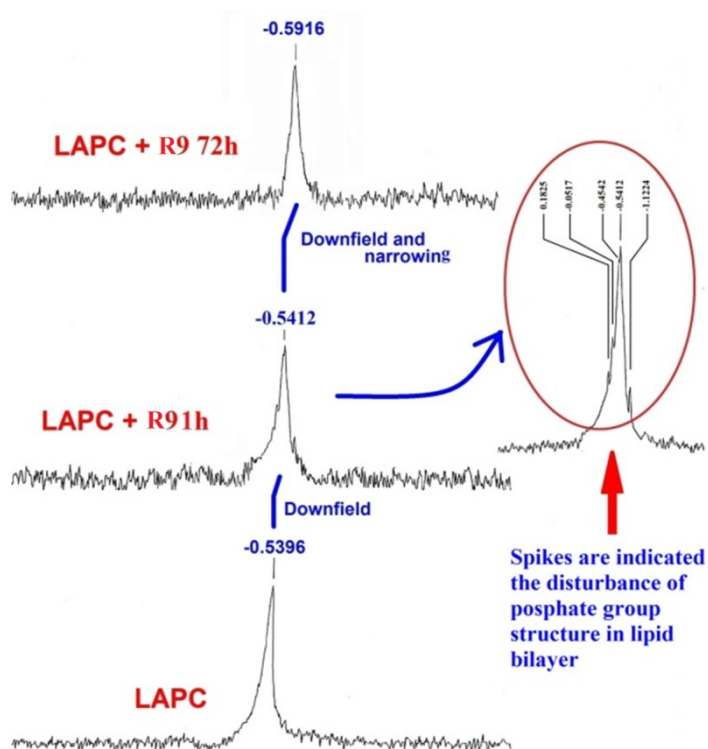


Fig. S18 ^{31}P NMR spectra of LIPC Vesicle in the presence and absence of R9.

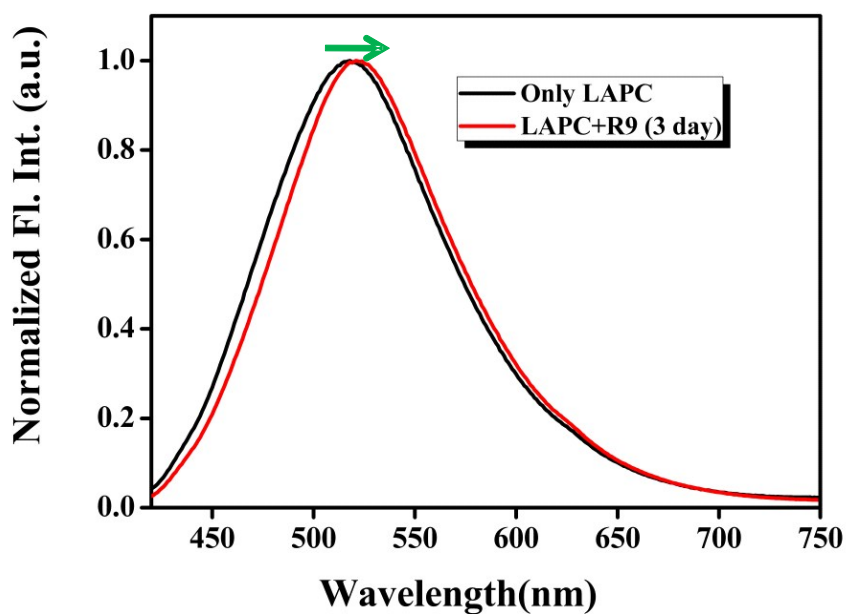


Fig. S19 Steady state emission spectra of C-153 in LAPC Vesicles in absence and presence of CPPs (R9) (30 μ M) (3days).

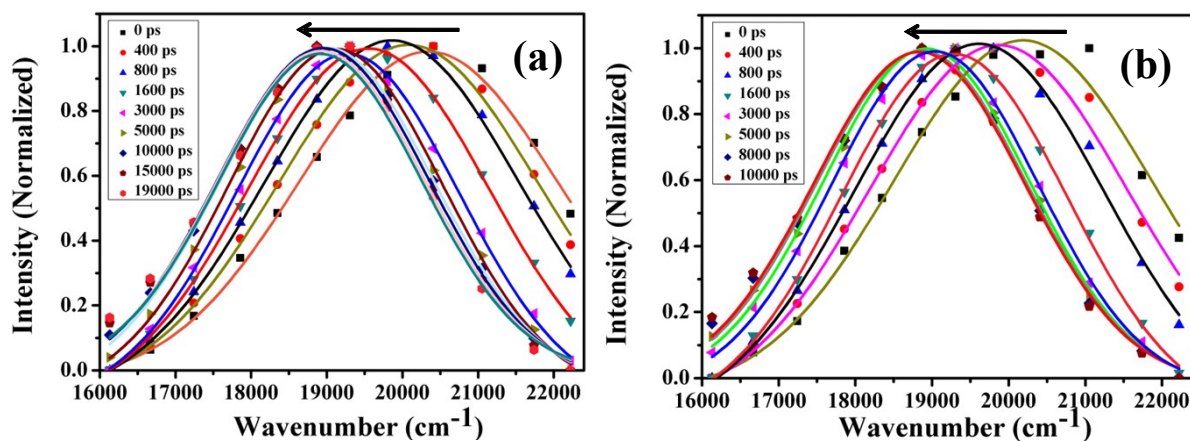


Fig. S20 Time resolved emission spectra (TRES) of C-153 in LAPC Vesicles in (a) absence and (b) presence of CPPs (R9) (30 μ M) (3days).

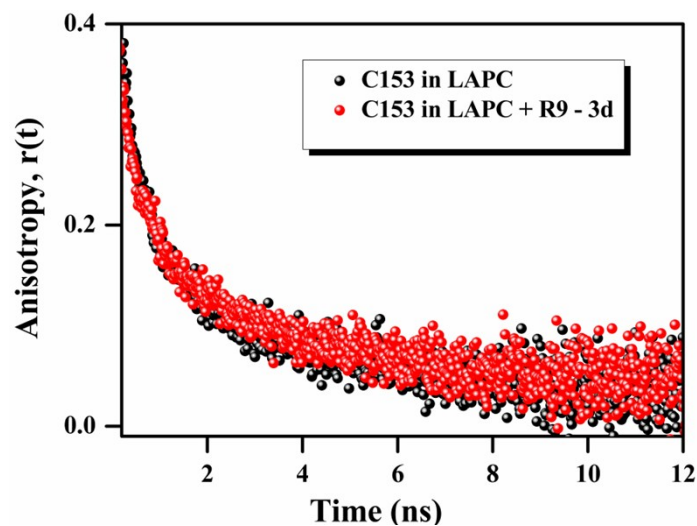


Fig. S21 Fluorescence anisotropy decays $[r(t)]$ of C153 inside different microenvironments of LAPC vesicle in the absence and presence of CPPs (R9) (30 μ M) ($\lambda_{ex} = 402$ nm).

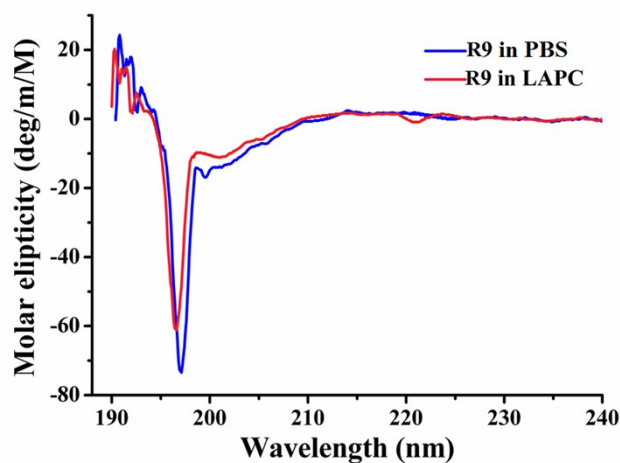


Fig. S22 Circular dichroism (CD) spectra of R9 in PBS and in LAPC.

References:

1. Liposomes: A practical approach; New, R. R. C., Ed., Oxford University Press: Oxford, England, **1990**; *p63*.
2. S. Ghosh, A. Roy, D. Banik, N. Kundu, J. Kuchlyan, A. Dhir and N. Sarkar, *Langmuir* 2015, **31**, 2310.
3. Fluorescence Microscopy: From Principles to Biological Applications. Edited by Ulrich Kubitscheck, WWW.wiley.com/wiley-Blackwell.